

# Revenue Maximization of Multi-class Charging Stations with Opportunistic Charger Sharing

Kihong Ahn\*, Aresh Dadlani<sup>†</sup>, Kiseon Kim\*, and Walid Saad<sup>‡</sup>

\* School of Electrical Engineering and Computer Science, GIST, Gwangju, South Korea

<sup>†</sup> Department of Electrical and Electronic Engineering, Nazarbayev University, Astana, Kazakhstan

<sup>‡</sup> Wireless@VT, Bradley Department of Electrical and Computer Engineering, Virginia Tech, Blacksburg, VA, USA

Email: {gandio, kskim}@gist.ac.kr, aresh.dadlani@nu.edu.kz, walids@vt.edu

**Abstract**—Distribution of limited smart grid resources among electric vehicles (EVs) with diverse service demands in an unfavorable manner can potentially degrade the overall profit achievable by the operating charging station (CS). In fact, inefficient resource management can lead to customer dissatisfaction arising due to prolonged queueing and blockage of EVs arriving at the CS for service. In this paper, a dynamic electric power allocation scheme for a charging facility is proposed and modeled as a bi-variate continuous-time Markovian process, with exclusive charging outlets being allotted to EVs of different classes in real-time. The presented mechanism enables the CS to guarantee the quality-of-service expected by customers in terms of blocking probability, while also maximizing its own overall revenue. By adopting a practical congestion pricing model within the defined profit function, the revenue optimization framework for a single CS is further extended to a load-balanced network of CSs. Simulation results for the single CS and networked models reveal considerably higher satisfaction levels for congested fast charging EV customers and improved attainable system revenue as compared to a baseline scenario which assumes no classification based on EV service preferences.

**Index Terms**—Electric vehicle charging model, continuous-time Markov chain, revenue maximization, shared chargers.

## I. INTRODUCTION

Perceptible advancement of battery and converter technologies over recent years has stimulated the large-scale penetration of plug-in electric vehicles (EVs) as eco-friendly and cost-efficient substitutes in the transportation sector. With threefold increase in global EV sales since 2013, a soaring 42% (i.e. over 773,600 units) was recorded in 2016 alone [1]. Amid the growth of EV market shares and energy policy regulations worldwide, EV charging operations are foreseen to pose new challenges for demand response management in smart grids [2]–[4]. A key issue in this line concerns devising optimal energy management paradigms that meet the expectations of customers with different service preferences without over-exploiting the limited resources and thus, jeopardizing the stability of power grids. To avert potential supply-demand imbalances arising due to the growing engagement of EVs, it is thus crucial to address and control factors impacting the performance limits of power supply infrastructures.

Customer satisfaction, in terms of waiting time and blocking probability, is the foremost performance measure mostly regarded in the EV charging decision process [5]. Depending on the queueing discipline and service distribution, a few

number of seminal studies aim at maximizing the profit of a charging station (CS) by minimizing the penalty associated with delayed and evicted EVs [6]–[8]. Despite the efforts made to meet service-level agreements (SLAs), the works referred above mandate all EVs arriving at a CS to enter a waiting space prior to commencing service. Nonetheless, as usually witnessed in conventional gas stations, an impatient EV customer may prefer to be blocked on arrival (finding no idle charging outlet) rather than to be delayed in queue for service [9]. Early blockage of such EV owners permits them to either retry after some random time period or visit another CS in local proximity thus, eliminating the waiting cost incurred.

Intertwined with customer satisfaction is the strategy various CS operators undertake to allocate scarce grid resources. The non-trivial revenue maximization problem becomes even more challenging when accommodating EVs with different battery charging specifications and profiles (AC Level-1, AC Level-2, DC Fast) [10], [11]. While more recent works consider either dedicated or shared resource pools in determining the utility of the charging network [12]–[14], theoretical aspects of an opportunistic sharing-based charger provisioning strategy under energy constraints have yet to be scrutinized.

Building on the premise of immediate resource allocation to EVs upon arrival, this paper introduces a novel real-time scheme for allocating shareable chargers to EVs subject to distinct service needs by taking their incoming traffic rates into account. To our best knowledge, all existing works allocate CS chargers to EVs based on the simple first-come-first-served sharing strategy. In contrast, here, we propose an efficient, opportunistic charger allocation strategy in a bufferless CS model that favors fast charging over slow charging requests during congestion in both, single and networked CS settings. Our results reveal higher attainable system revenue as compared to the baseline counterpart which does not classify EV service requests. In that course, our main contributions are:

- Continuous-time Markov chain (CTMC) characterization of a dynamic resource allocation scheme for a single CS with two EV service classes (i.e. slow and fast).
- Optimal revenue framework formulation for the multi-class CS model using an amended pricing function to alleviate congestion and meet quality-of-service (QoS) expectations of EV customers.
- Network-level performance analysis of multiple CSs me-

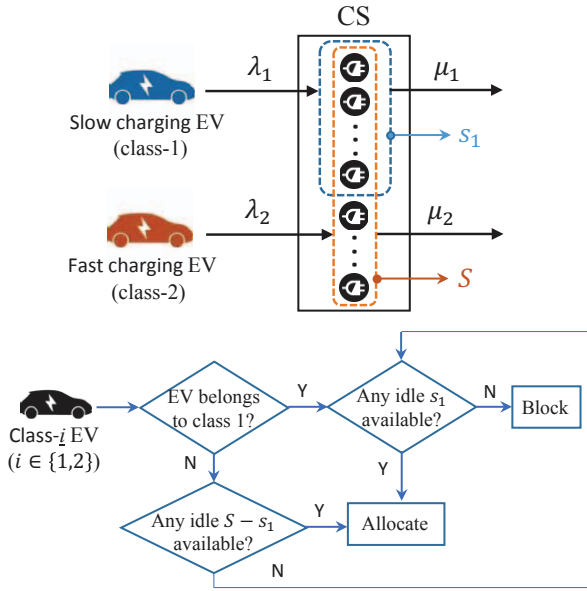


Fig. 1: Schematic design and charger allocation strategy of a two-class charging model.

diated by a centralized load dispatching entity and simulation comparison with an undifferentiated single-class baseline model under varying traffic intensities.

The rest of this paper is organized as follows. The proposed performance model for a single CS is presented in Section II, followed by details on the revenue maximization formulation with an effective pricing mechanism in Section III. Section IV discusses the optimal resource allocation scheme for a network of multiple CSs. Numerical simulations and discussions follow in Section V. Finally, Section VI concludes the paper.

## II. SINGLE CS SYSTEM MODEL

We consider a CS facility equipped with  $S$  charging outlets capable of charging  $M = 2$  service-differentiated classes of EVs. The CS is inflexible in meeting additional demands as it is assumed to draw  $S$  discretized units of constant power from the grid. In other words, the CS reaches its maximum capacity when all the charging outlets are busy. For  $i \in \{1, 2\}$ , EVs of class  $i$  are assumed to follow a Poisson arrival with rate  $\lambda_i > 0$  and exponentially distributed customer service time with mean  $\mu_i^{-1} > 0$ . To account for the diversity range in slow and fast charging requests, EVs belonging to classes 1 and 2 are allocated  $s_1$  and  $s_2$  chargers at any given time, respectively, such that  $s_1 < s_2 \leq S$  when class-2 has non-preemptive priority in using the charger outlets of class-1. Given these notations and assumptions, the single CS model can thus, be expressed as a finite-space CTMC  $\{X(t), t \geq 0\}$ .

To capture the state of the system for  $M=2$  at time  $t$ , we define  $N_1(t)$  and  $N_2(t)$  as the number of class-1 and class-2 EVs being served by the system at time  $t$ , respectively. Without loss of generality, we consider class-2 to have service priority over class-1. An EV of class 2 is allocated one of the  $s_1$  outlets only if (i) all  $S-s_1$  outlets are occupied by other class-2 EVs

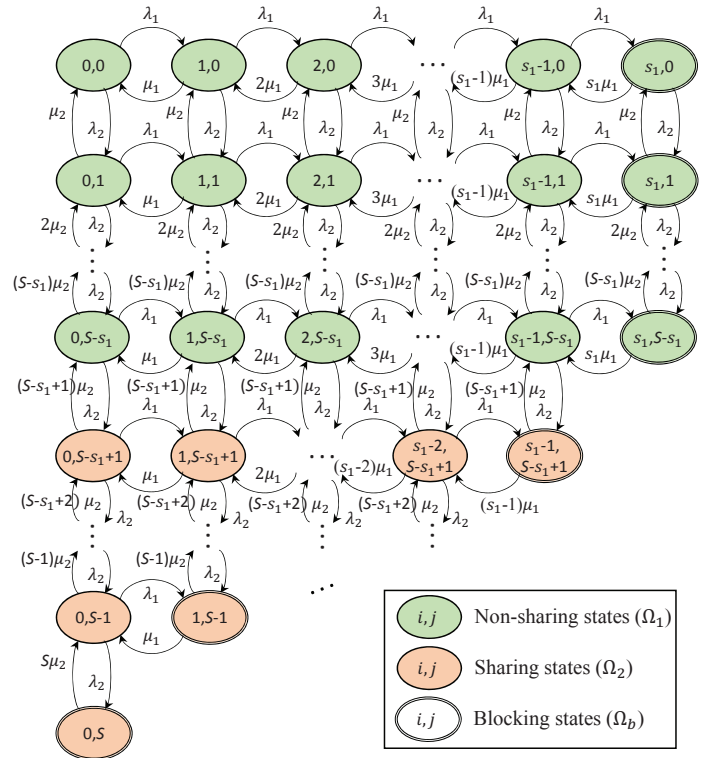


Fig. 2: Markovian two-class charging model representation.

and (ii) at least one of the  $s_1$  outlets is idle. Subsequently, the system in Fig. 1 can be characterized by a bi-variate process  $X(t) = (N_1(t), N_2(t))$  taking values in the state space  $\Omega = \{(i, j) | 0 \leq i \leq s_1, j \leq S - i\}$ , where  $|\Omega| = \sum_{k=0}^{s_1} (S+1-k)$ . For the corresponding birth-death process shown in Fig. 2, the transition from some state  $x = (i', j') \in \Omega$  to any adjacent state  $y \in \Omega$  occurs at the following rates:

$$q_{x,y} = \begin{cases} \lambda_1, & \text{if } y = (i'+1, j'); i' < s_1; j' < S-1-i', \\ \lambda_2, & \text{if } y = (i', j'+1); i' < s_1; j' < S-1-i', \\ i' \mu_1, & \text{if } y = (i'-1, j'); 1 \leq i' \leq s_1; j' \leq S-i', \\ j' \mu_2, & \text{if } y = (i', j'-1); i' \leq s_1; 1 \leq j' \leq S-i', \\ 0, & \text{if otherwise.} \end{cases} \quad (1)$$

These rates can be re-arranged in matrix form as elements of the infinitesimal generator matrix  $Q : \Omega \times \Omega \rightarrow \mathbb{R}$  such that:

$$Q_{|\Omega| \times |\Omega|} = \begin{cases} q_{x,y}, & \text{if } x \neq y \\ -\sum_{y \in \Omega} q_{x,y}, & \text{if } x = y. \end{cases} \quad (2)$$

Defining  $\Pi = [\pi_{i,j}]_{1 \times |\Omega|}$  as the steady-state probability vector, with each element  $\pi_{i,j}$  denoting the probability of having  $i$  number of class-1 and  $j$  number of class-2 vehicles in service at the CS, the linear system  $\Pi \cdot Q = 0$  and  $\Pi \cdot e = 1$  yields the following closed-form solution:

$$\pi_{i,j} = \frac{1}{i!j!} \left( \frac{\lambda_1}{\mu_1} \right)^i \left( \frac{\lambda_2}{\mu_2} \right)^j \pi_{0,0}, \quad (3)$$

where  $0 \leq i \leq s_1$ ,  $0 \leq j \leq S-i$ , and  $\pi_{0,0}$  is the normalized equation given by:

$$\pi_{0,0} = \left[ \sum_{i=0}^{s_1} \sum_{j=0}^{S-i} \frac{1}{i!j!} \left( \frac{\lambda_1}{\mu_1} \right)^i \left( \frac{\lambda_2}{\mu_2} \right)^j \right]^{-1}. \quad (4)$$

The blocking probability for each class can now be derived from the stationary probability distribution. An incoming EV of class-2 is blocked only if (i) all  $S-s_1$  chargers are occupied by other EVs of class-2 and (ii) the remaining  $s_1$  chargers are busy. Denoted by  $P_2$ , the blocking probability of class-2 EVs can be calculated as below:

$$P_2 = \sum_{i+j=S} \pi_{i,j} = \frac{\pi_{0,0}}{S!} \sum_{j=S-s_1}^S \binom{S}{j} \left( \frac{\lambda_1}{\mu_1} \right)^{S-j} \left( \frac{\lambda_2}{\mu_2} \right)^j. \quad (5)$$

Similar to (5), the blocking probability of a class-1 EV,  $P_1$ , includes an additional term associated with threshold  $s_1 < S$ :

$$P_1 = P_2 + \sum_{j=0}^{S-(s_1+1)} \pi_{s_1,j}. \quad (6)$$

As a result, the proportion of vehicles denied service due to blockage is denoted by  $\mathcal{N}_b$  and can be obtained as follows:

$$\mathcal{N}_b = \frac{\lambda_1}{\lambda_1 + \lambda_2} P_1 + \frac{\lambda_2}{\lambda_1 + \lambda_2} P_2. \quad (7)$$

### III. SINGLE CS REVENUE FORMULATION

The revenue earned by the operating CS can be quantified in terms of the charging model dynamics. As the power grid resources are shared instantaneously among EV owners willing to pay for services in accordance to their needs, the revenue function ( $\mathcal{R}$ ) is defined using three main cost components; the mean profit ( $f_P$ ), the mean blocking penalty ( $f_B$ ), and the mean maintenance cost ( $f_M$ ). To facilitate the definitions that follow, we divide the state space into two disjoint sub-spaces, such that for any given sub-space  $\Omega_m$ ,  $1 \leq m \leq M$ , the constituent system states correspond to cases when class- $m$  EVs are assigned idle chargers primarily reserved for EVs with lower service demands rather than being blocked from service. Let  $\Phi_m$  represent the set of class- $m$  idle chargers allocable to faster charging EVs that find all dedicated chargers occupied upon arrival. Thus,  $\Omega_m$  can be formally generalized as:

$$\Omega_m = \left\{ (i_1, \dots, i_m, \dots, i_M) \mid s_m < i_m \leq s_m + \sum_{r=1}^{m-1} |\Phi_r|, \right. \\ \left. 0 \leq i_{m+1} \leq s_{m+1}, \dots, 0 \leq i_M \leq S - \sum_{r=1}^{M-1} s_r \right\}. \quad (8)$$

#### A. Derivation of $f_P$

The overall profit made by the CS is differentiated according to the service grades of incoming EVs. For any state  $x \in \Omega$ , let  $n_x^m$  and  $\pi_x$  denote the number of class- $m$  EVs in state  $x$  and the stationary probability of being in  $x$ , respectively. Also, let  $p_m$  be the price paid by a class- $m$  EV for service; fast charging customers are required to pay more amount of money as compared to low charging customers [8], [9]. Subsequently, the average profit achievable for any  $M$  number of EV service classes is computed as:

$$f_P = \sum_{r=1}^M \left( p_r \sum_{x \in \Omega_r} n_x^r \pi_x \right). \quad (9)$$

#### B. Derivation of $f_B$

The average penalty incurred due to the blockage of a class- $m$  EV from service is given below, where  $c_m$  symbolizes the compensation cost reimbursed to the blocked EV customer and  $\Omega_b$  is the set of all blocking states exemplified in Fig. 2:

$$f_B = \sum_{r=1}^M \left( c_r \sum_{x \in \Omega_b} n_x^r \pi_x \right). \quad (10)$$

#### C. Derivation of $f_M$

Similar to [9], the final component in our revenue model is related to the subsidiary maintenance fees covering ancillary expenses (installation, labor, acquisition, etc.), with  $\bar{c}_0$  and  $\bar{d}_0$  taken to be positive constants:

$$f_M = \sum_{r=1}^M \left( \bar{c}_0 \sum_{x \in \Omega} n_x^r \pi_x \right) + \bar{d}_0 S. \quad (11)$$

#### D. Pricing Policies for $p_k$ and $c_k$

To comply with the customer QoS satisfaction level specified in the SLA, an adjustable pricing mechanism is needed to mitigate congestion of EV service requests at the CS without compromising the net revenue substantially. By extending the myopic pricing policy of [15] to our multi-class setting, we adopt the following principle in steady-state:

$$p_m = \begin{cases} \bar{p}_m, & \text{if } \lambda_m \leq \lambda_m^* \\ \bar{p}_m + \bar{p}_m \sqrt{-\log \left( \frac{\lambda_m^*}{\lambda_m} \right)}, & \text{if } \lambda_m > \lambda_m^*, \end{cases} \quad (12)$$

where  $\lambda_m^* \in [0, \lambda_m^{\max}]$  is the maximum arrival rate satisfying the QoS target denoted as  $\mathcal{N}_b^{\max}$  and  $\bar{p}_m$  is the normal charging price fixed by the CS operator. It is obvious that an arriving fast charging EV finding all chargers dedicated to its class busy is required to pay a relatively higher price to utilize an idle charger of a slower charging class, i.e.  $\forall i, j, k \in \{1, 2, \dots, M\}$ ,  $p_i \leq p_j \leq p_k$  if  $i < j < k$ . Likewise, since idle chargers of low charging classes are shared with EVs from higher classes opportunistically, we define the compensation cost to be  $c_m = \alpha p_m$  where  $\alpha \in [0, 1]$  is set by the CS operator.

Consequently, the total revenue of a single CS with multiple service classes is calculated as below:

$$\mathcal{R} = f_P - f_B - f_M. \quad (13)$$

Fig. 3 plots  $\mathcal{R}$  as function of  $S$  for three different  $(s_1, s_2)$  ratios in a single CS with  $M = 2$  service classes. The revenue model is evaluated for parameters  $(\lambda_1, \lambda_2) = (6, 6)$ ,  $(\mu_1, \mu_2) = (1, 3)$ ,  $(\bar{p}_1, \bar{p}_2) = (3, 4)$ ,  $\mathcal{N}_b^{\max} = 5\%$ ,  $(\lambda_1^{\max}, \lambda_2^{\max}) = (10, 10)$ ,  $\alpha = 0.7$ ,  $\bar{c}_0 = 0.1$ , and  $\bar{d}_0 = 0.02$ . The baseline is defined to be a single-class system with traffic intensity equal to the sum of the traffic intensities of customer classes 1 and 2, and  $s_1 = S$ . The blocking probability for such a system is thus, given as:

$$P_0 = \frac{\pi_{0,0}}{S!} \left( \frac{\lambda_1}{\mu_1} + \frac{\lambda_2}{\mu_2} \right)^S. \quad (14)$$

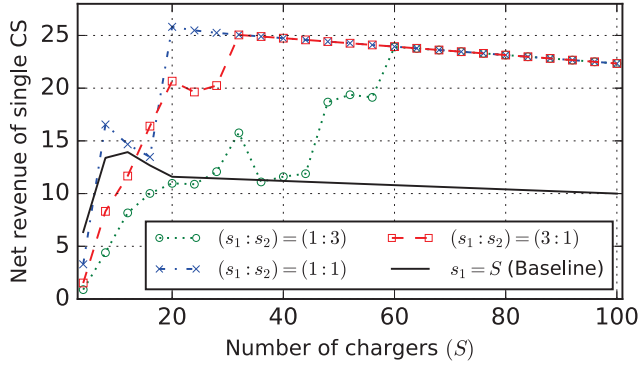


Fig. 3: Net revenue profile of a single CS in terms of  $S$  for a two-class charging scenario.

The existence of an optimal  $S$  value for which the net revenue peaks is evident in this figure. Moreover, the overall revenue for all three ratios converges as  $S$  increases. This is because abundance of chargers reduces the EV blocking probability.

#### IV. NETWORK-LEVEL RESOURCE ALLOCATION

In this section, we analyze the revenue maximization problem for a network of  $N$  closely-located CSs as in Fig. 4. We assume a central load dispatcher that distributes the incoming traffic to the most appropriate CS in a probabilistic manner. Higher resource utilization and real-time decision-making are the main advantages of a centrally operated load dispatcher [15]–[17]. Also, we use  $S_n$  to denote the number of chargers installed at station  $CS_n$ , where  $n \in \{1, 2, \dots, N\}$ . Based on the decomposition property of Poisson processes,  $\Lambda_i$  denotes a Poisson process with aggregated rate  $\sum_{n=1}^N \lambda_i^{(n)}$ , where the service requests arriving at  $CS_n$  are independent and follow a Poisson process with rate  $\lambda_i^{(n)}$ . As a result,  $\Lambda_i \geq \sum_{n=1}^N \lambda_i^{(n)}$ .

##### A. Undifferentiated Charging Requests

Serving as the baseline for our performance comparison, all EV service requests are considered to be equally prioritized in this case. In other words, chargers are allocated to EVs on a first-come-first-served basis irrespective of their service class thus, resulting in the following revenue maximization problem for the classless scenario:

$$\text{maximize}_{\{\lambda^{(n)}\}} \sum_{n=1}^N \lambda^{(n)} \mathcal{R}_n - \beta \left( \Lambda - \sum_{n=1}^N \lambda^{(n)} \right) \quad (15)$$

$$\text{subject to } P_0^{(n)} \leq \mathcal{N}_b^{\max} \quad \forall n \in \{1, 2, \dots, N\}, \quad (16)$$

$$\sum_{n=1}^N \lambda^{(n)} \leq \Lambda. \quad (17)$$

The first term in (15) reflects the aggregated network revenue, where  $\lambda^{(n)} \mathcal{R}_n$  is the fraction contributed by  $CS_n$ . The second term calculates the penalty associated with EVs blocked by the central dispatcher when overwhelmed by service requests. The fee  $\beta \in [0, 1]$  is decided by the central dispatcher authorized to decline service demands under high request rates. For the classless scenario, where  $s_1 = S$ ,  $P_0^{(n)}$  denotes the blocking probability of EVs arriving at  $CS_n$ .

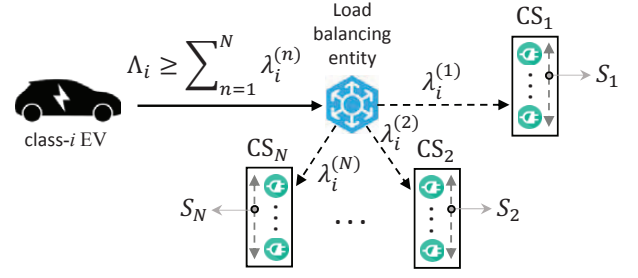


Fig. 4: Network of CSs governed by a central load dispatcher.

##### Algorithm 1 Centralized pricing-based load balancing

**Input:**  $N, \Lambda_r, \Delta\lambda, \beta_r, \mathcal{N}_b^{\max}, \bar{p}_r$ , where  $r \in \{1, 2, \dots, M\}$   
**Output:** Optimal  $\lambda_r^{(n)}$  values, corresponding net revenue  
1: Find all  $(\Lambda_r / \Delta\lambda + 1)^N$  permutations with step size  $\Delta\lambda$ .  
2: Discard invalid permutations that add up to more than  $\Lambda_r$ .  
3: **for** each valid permutation of class  $r$  **do**  
4:   **if**  $(\sum_{r=1}^M P_r^{(n)} \leq \mathcal{N}_b^{\max})$  and  $(\Lambda_r \geq \sum_{n=1}^N \lambda_r^{(n)})$  **then**  
5:      $\mathcal{R}_{net} \leftarrow$  Calculate revenue as in Section III  
6:     **if**  $\mathcal{R}_{net}$  is the maximum so far **then**  
7:        $\lambda_{r,n}^{opt} \leftarrow$  Save selected rate permutation.  
8:     **end if**  
9:   **end if**  
10: **end for**  
11: **for** each class  $r$  **do**  
12:    $B \leftarrow B + \beta_r (\Lambda_r - \sum_{n=1}^N \lambda_{r,n}^{opt})$   
13: **end for**  
14: **return**  $\lambda_{r,n}^{opt}, (\mathcal{R}_{net} - B)$

##### B. Differentiated Charging Requests

We now account for charger allocation in a setting where the central entity optimally distributes the service traffic of each class among the CSs so as to maximize the overall revenue. Unlike the baseline, the computational complexity of revenue optimization increases exponentially with the number of EV classes. The central entity executes Algorithm 1 to distribute the service requests to each CS in the network. The algorithm returns the optimal  $\lambda_i^{(n)}$  values that generates the maximum revenue. The revenue maximization framework for a network of  $N$  CSs is as follows, where  $\beta_i$  and  $P_i^{(n)}$  denote respectively, the eviction fee for class- $i$  ( $i \in \{1, 2, \dots, M\}$ ) and the blocking probability of class- $i$  EVs at  $CS_n$ :

$$\text{maximize}_{\{\lambda_r^{(n)}\}} \sum_{n=1}^N \sum_{r=1}^M \lambda_r^{(n)} \mathcal{R}_n - \sum_{r=1}^M \beta_r \left( \Lambda_r - \sum_{n=1}^N \lambda_r^{(n)} \right) \quad (18)$$

$$\text{subject to } \sum_{r=1}^M P_r^{(n)} \leq \mathcal{N}_b^{\max} \quad \forall n \in \{1, 2, \dots, N\}, \quad (19)$$

$$\sum_{n=1}^N \lambda_r^{(n)} \leq \Lambda_r \quad \forall r \in \{1, 2, \dots, M\}. \quad (20)$$

#### V. PERFORMANCE EVALUATION AND DISCUSSIONS

The proposed CS performance model is evaluated in terms of the charging blocking probabilities of each customer class

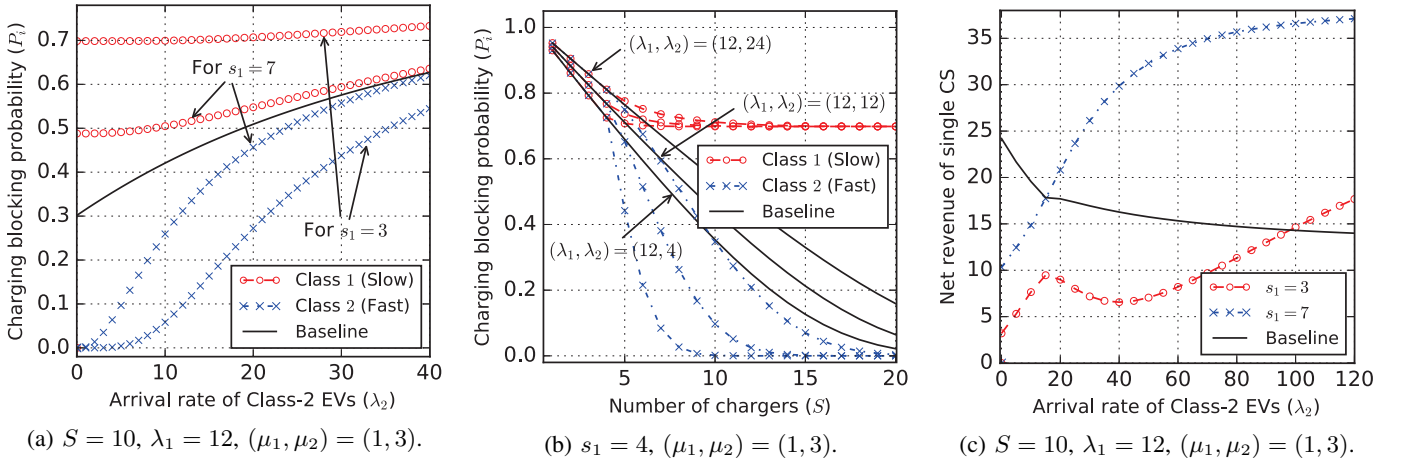


Fig. 5: Single CS performance evaluation: (a) charging blocking probability versus  $\lambda_2$ , (b) charging blocking probability versus  $S$ , and (c) net revenue versus  $\lambda_2$ .

and the net system revenue. For sake of better demonstration, we adopt the two-class model throughout this section. Unless stated otherwise, the parameters are set to be as in Fig. 3.

#### A. Single CS Performance Analysis

Fig. 5 illustrates the impact of various control parameters on the performance indicators in a single CS setting. In particular, Fig. 5a shows the blocking probabilities of each service class in terms of class-2 EV arrival rate. For lower values of  $\lambda_2$ , class-2 EVs experience a much lesser chance of service denial than the slow charging EVs of class-1. The blocking probabilities of the two classes however, converge towards the baseline mark as  $\lambda_2$  increases. Moreover, for smaller  $s_1$  values, newly arriving class-2 EVs are probable to find an idle charger from a larger set of dedicated chargers thus, yielding lower dissatisfaction of class-2 customers. For instance, the blocking probability of fast charging EVs rises by approximately 142% as  $s_1$  increases from 3 to 7 at  $\lambda_2 = 10$ . In contrast,  $P_1$  is reduced by 28.5% for the same  $\lambda_2$  value. Here, even though the satisfaction of class-1 customers are slightly compromised over class-2 customers, the overall satisfaction level determined as  $N_b^{\max}$  is still guaranteed. Nonetheless, such favoring behavior gradually fades away as  $\lambda_2$  increases.

In Fig. 5b, we observe the influence of the charger set size on the system blocking probability for varying EV arrival rates. Note that  $P_2$  reaches zero for a smaller set size of  $S = 10$  chargers when  $\lambda_1 > \lambda_2$ , while  $P_1$  stabilizes at 0.69. This figure reveals that the proposed charging model prioritizes congested fast-charging EVs over slow charging EVs as the number of installed chargers at the CS increases. In comparison to the baseline, our proposed strategy facilitates high charging EVs (who pay more) opportunistically by allocating them any idle  $s_1$ . Nonetheless, if a class-1 EV finds all  $s_1$  chargers occupied on arrival, it is unwillingly evicted for a compensation fee.

The net revenue earned by the CS under varying  $\lambda_2$  values is shown in Fig. 5c. Note that unlike the case of  $s_1 = 7$ , the revenue for  $s_1 = 3$  slightly decreases at  $\lambda_2 = 12$  before rising

up again. Such behavior for  $\lambda_2 \in [12, 40]$  can be explained based on the high  $P_1$  value used in Fig. 5a; the corresponding penalty paid for evicting class-1 EVs is higher than the profit made by accommodating congested class-2 EV customers. The total revenue however, beats the baseline scenario and peaks at an extreme value of  $\lambda_2 \approx 500$  (not shown in the figure).

#### B. Network-level Performance Analysis

We now evaluate the performance of our strategy in a networked environment comprising of  $N = 3$  identical charging stations with  $S = 5$  chargers each,  $N_b^{\max} = 0.25\%$ ,  $\Delta\lambda = 1$ ,  $\beta_r = 0.9$ ,  $(\lambda_1^{\max}, \lambda_2^{\max}) = (7, 7)$ , and  $(\mu_1, \mu_2) = (1, 2)$ . Table I summarizes the optimal EV arrival rates distributed among the three CSs by the central entity for which the maximum revenue is obtained considering the undifferentiated service class (Type A) and the differentiated service classes with  $s_1 = 2$  (Type B) and  $s_1 = 4$  (Type C).

The impact of dedicating chargers to specific service classes on the overall network revenue is manifold. Unlike the undifferentiated baseline model, Type B and Type C scenarios reveal reduction in the blocked fraction of fast charging EVs. In addition, while the baseline case outperforms its Type B counterpart in maximizing the net revenue, it is dominated by Type C where slow charging EVs are primarily allocated a larger number of installed chargers for service. On the other hand, Type B demonstrates a more evenly balanced service request load at the expense of evicting a fraction of the low charging EV arrivals to meet the SLA requirements. The revenue gap between Type A and Type B reduces as  $\Lambda_2$  becomes greater than  $\Lambda_1$ , which is in complete agreement with the results of Fig. 5. For instance, as  $\Lambda_2$  increases from 3 to 5, Type C yields almost 80% increase in revenue as compared to the baseline case. For  $(\Lambda_1, \Lambda_2) = (3, 5)$ , the system witnesses a revenue increase of 104.7%. This is merely due to the fact that congested fast charging EVs intrinsically tend to pay more to utilize a lower class charger rather than be declined service. Therefore, by dedicating a larger fraction of the charger set to

TABLE I: System performance and revenue comparison of Type A (undifferentiated service), Type B (differentiated service,  $s_1 = 2$ ), and Type C (differentiated service,  $s_1 = 4$ ) network scenarios.

$(\Lambda_1, \Lambda_2)$	Type	CS <sub>1</sub>			CS <sub>2</sub>			CS <sub>3</sub>			$\sum_{n=1}^3 \mathcal{R}_n$
		$(\lambda_1^{(1)}, \lambda_2^{(1)})$	$\mathcal{R}_1$	$(P_1, P_2)$	$(\lambda_1^{(2)}, \lambda_2^{(2)})$	$\mathcal{R}_2$	$(P_1, P_2)$	$(\lambda_1^{(3)}, \lambda_2^{(3)})$	$\mathcal{R}_3$	$(P_1, P_2)$	
(5,3)	A	(2,0)	2.4046	(0.0367,0.0367)	(1,2)	2.4046	(0.0367,0.0367)	(2,1)	2.7899	(0.0697,0.0697)	7.599
	B	(1,1)	1.7084	(0.2004,0.0032)	(1,1)	1.7084	(0.2004,0.0032)	(1,1)	1.7084	(0.2004,0.0032)	3.3252
	C	(3,0)	2.2687	(0.2061,0)	(0,3)	7.5737	(0.0142,0.0142)	(2,0)	1.9333	(0.0952,0)	11.7758
(5,5)	A	(3,0)	3.06	(0.1101,0.1101)	(0,5)	4.9487	(0.0697,0.0697)	(2,0)	2.4046	(0.0367,0.0367)	10.4133
	B	(1,2)	2.7867	(0.2047,0.0197)	(1,2)	2.7867	(0.2047,0.0197)	(1,1)	1.7084	(0.2004,0.0032)	5.4819
	C	(3,0)	2.2687	(0.2061,0)	(0,5)	14.6296	(0.0697,0.0697)	(2,0)	1.9333	(0.0952,0)	18.8316
(3,5)	A	(1,0)	1.2796	(0.0031,0.0031)	(2,0)	2.4046	(0.0367,0.0367)	(0,5)	4.9487	(0.0697,0.0697)	8.6329
	B	(1,2)	2.7867	(0.2047,0.0197)	(1,1)	1.7084	(0.2004,0.2004)	(1,2)	2.7867	(0.2047,0.2047)	7.2819
	C	(1,0)	1.1138	(0.0154,0)	(2,0)	1.9333	(0.0952,0)	(0,5)	14.6296	(0.0697,0.0697)	17.6768

slow charging EV customers, the proposed allocation strategy generates more revenue while guaranteeing the satisfaction expectation of customers belonging to both service classes. Imposing a stricter QoS level would distribute the incoming service load more evenly, while generating lower revenue due to EVs blocked by the load balancer.

## VI. CONCLUSION

In this paper, we have proposed a novel congestion pricing-based resource allocation model for electric vehicle charging stations accommodating customers with distinct service preferences in real-time. The presented charger sharing strategy was formulated using a multi-dimensional Markovian chain to attain the maximum possible revenue for a single as well as network of charging stations. In comparison to the single-class undifferentiated system set-up, the out-performance of the proposed strategy in terms of blocking probability and system revenue maximization was confirmed via simulation results. Service classes permitted to non-preemptively utilize chargers primarily reserved for slower EV charging classes experience lower service eviction as compared to the classless baseline. An interesting follow-up on this work would involve analysis of the intrinsic retrial behavior of blocked EV owners who randomly attempt to access grid resources and its impact on various performance indicators under several system configurations. In addition, finding the optimal number of chargers allocable to each class under different EV traffic intensities would provide better insights on the system model behavior and deployment cost estimate.

## ACKNOWLEDGMENT

This work was supported by the GIST Research Institute (GRI), South Korea, in 2017 and, in part, by the US National Science Foundation (NSF) under Grant ECCS-1549894.

## REFERENCES

- [1] (2017, March 29). *EV-Volumes - The Electric Vehicle World Sales Database*. [Online]. Available: <http://www.ev-volumes.com>
- [2] A. Shortt and M. O'Malley, "Quantifying the long-term impact of electric vehicles on the generation portfolio," *IEEE Trans. Smart Grid*, vol. 5, no. 1, pp. 71–83, Jan. 2014.
- [3] J. S. Vardakas, N. Zorba, and C. V. Verikoukis, "A survey on demand response programs in smart grids: pricing methods and optimization algorithms," *IEEE Commun. Surveys Tuts.*, vol. 17, no. 1, pp. 152–178, Jul. 2014.
- [4] P. Samadi, V. W. S. Wong, and R. Schober, "Load scheduling and power trading in systems with high penetration of renewable energy resources," *IEEE Trans. Smart Grid*, vol. 7, no. 4, pp. 1802–1812, Jun. 2015.
- [5] S. R. Etesami, W. Saad, N. B. Mandayam, and H. V. Poor, "Smart routing in smart grids," in *Proc. IEEE Conference on Decision and Control (CDC)*, Dec. 2017.
- [6] D. Said, S. Cherkaoui, and L. Khoukhi, "Multi-priority queuing for electric vehicles charging at public supply stations with price variation," *Wirel. Commun. Mob. Comput.*, vol. 15, no. 6, pp. 1049–1065, Apr. 2015.
- [7] P. Fan, B. Sainbayar, and S. Ren, "Operation analysis of fast charging stations with energy demand control of electric vehicles," *IEEE Trans. Smart Grid*, vol. 6, no. 4, pp. 1819–1826, Jul. 2015.
- [8] C. Kong, I. S. Bayram, and M. Devetsikiotis, "Revenue optimization frameworks for multi-class PEV charging stations," *IEEE Access*, vol. 3, pp. 2140–2150, Nov. 2015.
- [9] I. S. Bayram, G. Michailidis, M. Devetsikiotis, and F. Granelli, "Electric power allocation in a network of fast charging stations," *IEEE J. Sel. Areas Commun.*, vol. 31, no. 7, Jul. 2013.
- [10] I. S. Bayram, M. Abdallah, and K. Qaraqe, "Providing QoS guarantees to multiple classes of EVs under deterministic grid power," in *Proc. IEEE International Energy Conference (ENERGYCON)*, May 2014, pp. 1403–1408.
- [11] X. Tan, B. Sun, and D. H. K. Tsang, "Queueing network models for electric vehicle charging station with battery swapping," in *Proc. IEEE International Conference on Smart Grid Communications (SmartGridComm)*, Nov. 2014, pp. 1–6.
- [12] I. S. Bayram, G. Michailidis, M. Devetsikiotis, F. Granelli, and S. Bhat-tacharya, "Smart vehicles in the smart grid: challenges, trends, and application to the design of charging stations," in *Control and Optimization Methods for Electric Smart Grids*, vol. 3, A. Chakraborty and M. D. Ilić, Eds. New York, NY, USA: Springer-Verlag, 2012, ser. Power Electronics and Power Systems, pp. 133–145.
- [13] M. Yilmaz and P. T. Krein, "Review of battery charger topologies, charging power levels, and infrastructure for plug-in electric and hybrid vehicles," *IEEE Trans. Power Electron.*, vol. 28, no. 5, pp. 2151–2169, May 2013.
- [14] M. C. Falvo, D. Sbordone, I. S. Bayram, and M. Devetsikiotis, "EV charging stations and modes: international standards," in *Proc. International Symposium on Power Electronics, Electrical Drives, Automation and Motion (SPEEDAM)*, Jun. 2014, pp. 1134–1139.
- [15] I. S. Bayram, G. Michailidis, I. Papapanagiotou, and M. Devetsikiotis, "Decentralized control of electric vehicles in a network of fast charging stations," in *Proc. IEEE Global Communications Conference (GLOBE-COM)*, Dec. 2013, pp. 2785–2790.
- [16] Z. Ma, D. S. Callaway, and I. A. Hiskens, "Decentralized charging control of large populations of plug-in electric vehicles," *IEEE Trans. Control Syst. Technol.*, vol. 21, no. 1, Jan. 2013.
- [17] M. G. Vayá and G. Andersson, "Plug-in electric vehicle charging approaches: centralized versus decentralized and strategic versus cooperative," in *Proc. IEEE Eindhoven PowerTech*, 2015, pp. 1–6.